# Experimental and Numerical Attenuation of Vibration for Delta Wing Using PI Controller

**Ahmed A. Ali**
Mechanical Eng. Dep.
Baghdad University
ahmedrobot65@yahoo.com

**Hussain Y. Mahmood**
Mechanical Eng. Dep.
Baghdad University
Hussain_Yousif2001@yahoo.com

**Mahmood Wael Saeed**
Mechanical Eng. Dep.
Baghdad University
mahmoodwael@rocketmail.com

## Abstract

Active vibration controlling loop with proportional - Integral (PI) controller was tested numerically and experimentally for delta wing with three different manufacturing materials; aluminum, [0/90] composite and aluminum foam, both P and PI loop were tested separately. Numerical work was performed in ANSYS v.15 where controller with piezoelectric transducers was totally integrated in program *macro*. Experimental wings where fabricated to be tested under simulated excitation. Labview 2015 program with high speed Data acquisition were used besides actuators to perform controlling circuit experimentally. Good suppression in wing oscillation was performed where 72% of wing's time of vibration was eliminated for aluminum foam wing. Noticeable agreement was achieved between experimental and numerical responses.

**Keywords:** Active vibration control, Delta wing, proportional - Integral (PI), ANSYS, Labview

## 1. Introduction

Active vibration control (AVC) is defined as a technique to attenuate undesired vibration. It is controlled by applying a counter force that is reversed to original force, but equal in amplitude to the original vibration to achieve the desired response. As a result two counter forces cancel each other and structure become steady state. Active vibration control is a modern approach in respect of vibration control at various places. The classic control technique is becoming too large for modern machine where space is limited and regular maintenance is not possible and if possible, it is too expensive, at such conditions AVC techniques comes handy, it is very cheap requires no manual maintenance and the life expectancy is also much more than the passive control **[1]**. AVC makes use of smart structure. In reference **[2]** worked on controlling of vibration for the single link arm which was modeled as cantilever beam. The studied arm was made from composite material with [0/90] lay-ups. Frist three modes of vibration were targeted to reduce the vibration of arm's end by using finite element analysis via ANSYS program besides experimental work. To reduce the arm's end oscillation the authors worked on introducing the profile of velocity by recording residual vibrations of arm and tacking root mean square (RMS) for the recorded values it was observed that decreasing of the 1st mode vibration playing a major role on residual vibration. The authors noticed that the residual vibrations of arms can be manipulated or reduced by selecting the best deceleration time in both trapezoidal and triangular velocity inputs. Authors in **[3]** tested the performance of Minimum actuation, power (MAP) technique as an AVC method, where MAP is a new control method works on minimizing voltage feuded to structure by visualizing and controlling powers of control references. Implementation of MAP was done theoretically and experimentally on simply supported aluminum plate with piezoelectric transducers (PZT), where main actuators used to excite the tested structure while subaltern actuators were used to vibration suppression. In this method PZT easily used to evaluate input power via measuring the electrical voltage without using sensors to decrease the error. The MAP theory also can be used for multi-frequency excitation. Authors of reference **[4]** utilized H∞ controlling method with a system of piezoelectric transducers in MATLAB software in which controlling process was performed. Authors of reference **[5]** studied different laminated theories and laminated existing model for active vibration control strategies by comparing fundamental frequencies and center deflection of each model to decide which techniques was the best in controlling. Authors of **[6]** presented an analytical model of sandwich beam and tested for modal analysis, with validation of results by simulating similar model in ABAQUS software. In reference **[7]** a sandwich beam was tested to suppress its overall vibration by means of LQR controlling strategy. Active vibration control of smart composite plate was presented by reference **[8]** (where they presented AVC with using two types of controlling techniques which were LQR and classical negative velocity feedback respectively. Authors of reference **[9]** studied sandwich beam with aluminum foam by simulating it in ABAQUS, PZT was used to test the effectiveness of using passive position feedback method. PID, velocity feedback and acceleration feedback controlling techniques were also utilized in active vibration suppression for aircraft wing in references **[10-13]**.

## 2. Analytical Presentation

### 2.1 PID Controller

Proportional – Integral – Derivative controller or what mentioned by PID represents one of the most famous regulators with output return signal. PID regulator was an important and most effective tool for controlling of many industrial processes. Nowadays the using of PID is developed to be used in about ninety five percent from most controlling circuits. Also high percentage of using PI regulator was noticed were it serves more effectively than using PID terms. Such types of regulators can be satisfied by using them in an individual container or by integrating them with other circuits to be work together. Also more accuracy and intelligence for PID actions can be satisfied by cooperation their performance with logic loop, selector, modern controlling strategy for example model predictive control. The main objective of such controller is to decrease as much as possible the error with time. Many researches were used PID controller for vibration suppression for different processes. In the present work PI controller was used as an effective tool for attenuating of vibration by using piezoelectric transducers as actuator. Selection of controller parameters affect in such a manner on adding more deterioration in response that needed to be controlled. PID algorithm is described by**[10]**:

$$u(t) = K\left(e(t) + \frac{1}{T_i}\int_0^t e(t)dt + T_d\frac{de(t)}{dt}\right) \qquad (1)$$

Where *u(t)* is the control signal and *e(t)* is the control error(e(t))= reference input(r(t)) – feedback(y(t)). The reference variable is often called the set point. The control signal is thus a sum of three terms: the P term is proportional to the error e(t), the I term is proportional to the integral of the error e(t), and the D term is proportional to the derivative of the error e(t). The controller parameters are the controller gain *K*, integral time *Ti*, and derivative time *Td* **[14]** Block diagram of PI control is shown in figure (1)

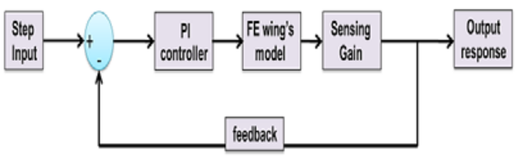


**Figure 1:** Block diagram of PI controlling loop

## 3. Finite Element Model

Wing construction was started by creating three keypoint by [Kp] command and then [L] command was used to connect those keypoint, after that [al] command was used to create the wing horizontal section as shown in figure (2).

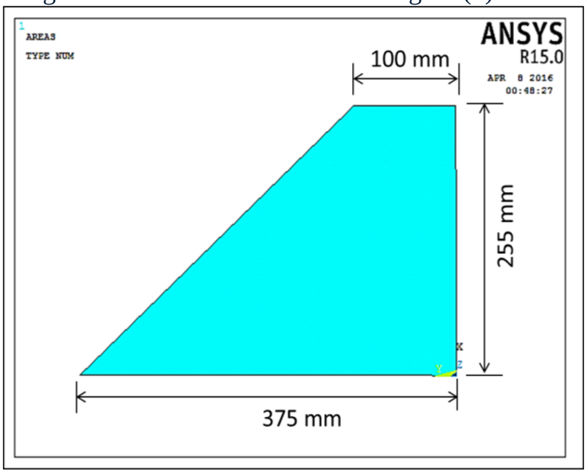


**Figure 2:** Finite element model

Many types of element can be utilized to mesh the studied model some of those elements are SHELL 181,SOLID 45 for volume, SOLID 46, but in order to keep this simulation simple and effective, shell 181 element type was selected to mesh the model where the structure was modeled as single layer of 0.4mm for Aluminum model, and two layer with thickness of 0.2mm for each layer of symmetric laminated glass epoxy composite [45/-45].layers were defined by using [SECDATA] command in which the angle of each layer was defined with its thickness.

Shell 181 is a four-node element with six degrees of freedom at each node: translations in the x, y, and z directions, and rotations about the x, y, and z-axes. It can be used for layered applications for modeling composite shells or sandwich construction meshed model is shown in figure .3. **[15]**

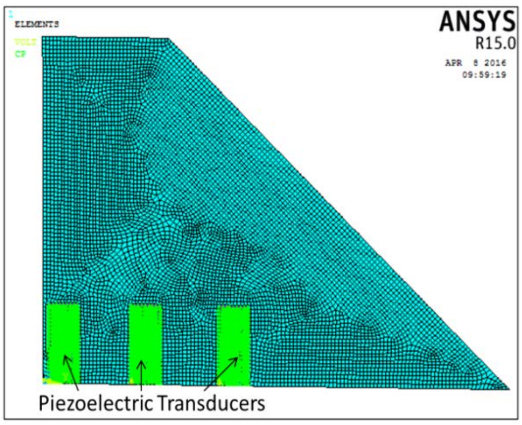


**Figure 3:** Meshing of finite element

Now piezoelectric patches must be defined in ANSYS with element has a coupling feature by which one can couple between both electrical and mechanical fields. So SOLID5 was used to mesh piezoelectric transducers of this study. This type of elements has 3-D magnetic, thermal, electric, piezoelectric, and the structural field capability with limited coupling between the fields. The element has eight nodes with up to six degrees of freedom at each node. Scalar potential formulations (reduced RSP, difference DSP, or general GSP) are available for modeling magneto static fields in a static analysis. When used in structural and piezoelectric analyses, SOLID5 has large deflection and stress stiffening capabilities.

Actuator's positions were identified based on maximum strain theory.

Modeling of piezoelectric material is given by their constitutive equations as **[4]**:

$\{T\} = [c]\{s\} - [e]\{E\}$ (5)

$\{D\} = [e^T]\{S\} + [\varepsilon]\{E\}$ (6)

Where mechanical variables T and S are stress and strain vectors; electrical variables D and E are electrical displacement and electric field vectors, respectively. Matrices [c], [e] and $[e^T]$ are piezoelectric material properties, where [c] is the elasticity matrix, [e] is the piezoelectric matrix and $[e^T]$ is the dielectric matrix. The equations of motion for the coupled piezoelectric can be expressed in terms of nodal quantities **[4]**,

$[M]\{\delta\} + [C]\{\delta\} + [K]\{\delta\} + [k^z]\{v\} = \{F\}$ (7)

$[k^z]^T\{\delta\} + [k^d]\{V\} = \{L\}$ .. (8)

Where [M] is the mass matrix derived from density and volume, [K] is the mechanical stiffness matrix derived from elasticity matrix, $[K^z]$ is the piezoelectric stiffness matrix derived from piezoelectric matrix, $[K^d]$ is the dielectric stiffness matrix derived from dielectric matrix, {u} and {V} are the vectors of nodal displacements and electrical potentials, {F} and {L} are the vectors of mechanical force and charge, respectively.

In this work three piezoelectric patches were distributed on the upper surface of tested wing, PPA-1001, PZT-5H was modeled with dimensions [54.4x22.4x0.46] mm similar to real dimensions. Dimensions of the studied delta wing are shown in figure (2)

Scooped view of the real piezoelectric actuator model is shown in figure (4) with its dimension. The coupling between both upper and lower nodes of patches was performed with ANSYS. Material properties of Aluminum and composite of [0/90] are listed in with material properties of PPA-1001 piezoelectric transducer produced by (MIDE) are listed in **Table .1**.

**Table .1:** Mechanical properties [16]

| Piezoelectric actuator | Epoxy-glass composite |
|---|---|
| ρ =7350 kg/$m^3$<br>Piezoelectric strain matrix (C/$m^2$)<br>E31 = 6.5×$10^9$<br>E33 = 23.3×$10^9$<br>E15 = 17×$10^9$<br>Elastic stiffness matrix (N/$m^2$)<br>C11 = 12.6<br>C12 = 7.95 | ρ =1830 kg/m³<br>Ex = 40.51 GPa<br>Ey = 13.96 GPa<br>Ez = 13.96 GPa<br>Gxy = 3.1 GPa<br>Gyz = 1.55 GPa<br>Gxz = 3.1 GPa<br>νxy = 0.22<br>νyz = 0.11<br>νxz = 0.22 |
| C13 = 8.41 | Aluminum |
| C33 = 11.7<br>C44 = 2.33<br>Dielectric matrix (F/m)<br>e11 = 1.503×$10^{-9}$ | ρ =2720 kg/m³<br>$\nu_{xy}$ = 0.33<br>E=69 GPa |
| e22 = 1.503×$10^{-9}$ | Aluminum foam |
| e33 = 1.3×$10^{-9}$ | ρ =460 kg/m^3<br>$\nu_{xy}$=0.34<br>E=110 MPa |

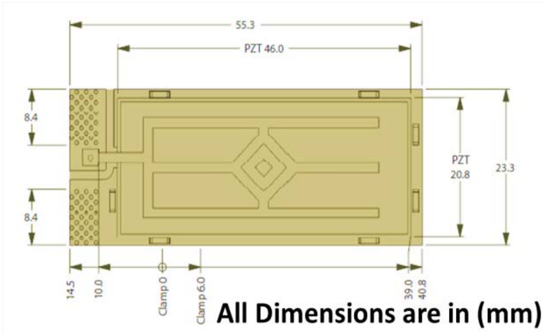


**Figure 4:** PPA-1001 Actuator

## 4. Experimental Model

Typical delta wing was modeled with .IGES extension, then it was exported with .ESP extension. Cutting was performed on AL plate with thickness of 0.5mm by SKYCNC2412 with dimensions similar to those used in numerical simulation as illustrated in figure (5) in which total aluminum wing is presented. Aluminum foam and composite delta wing used in experimental work were also fabricated and presented in figures (6) & (9) respectively.

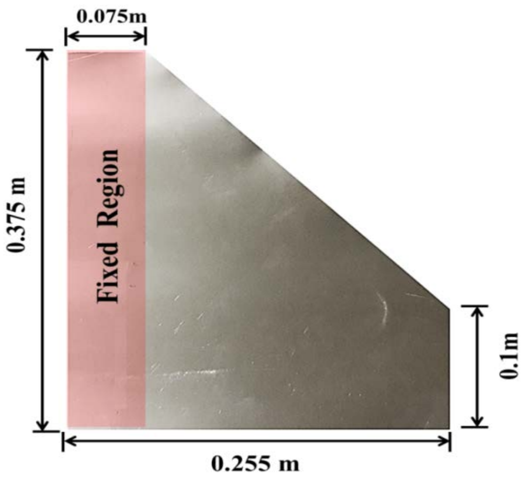


**Figure 5**: Typical Aluminium delta wing

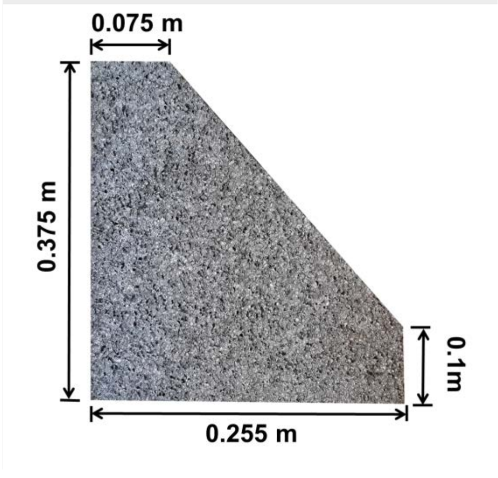


**Figure 6:** Typical aluminium foam delta wing


**Figure 7:** Mold for composite delta wing

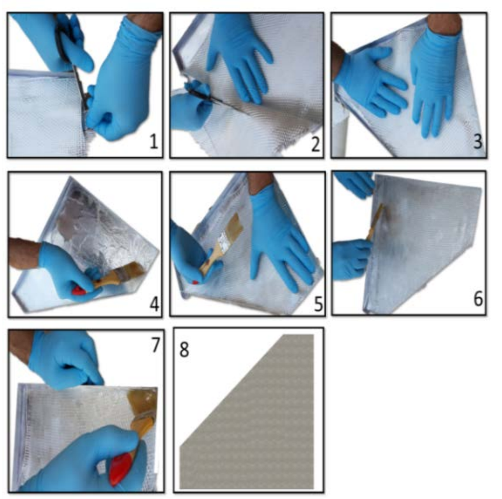


**Figure 8:** Manufacturing process of composite delta wing

Final [0/90] composite delta wing is presented in figure (9)

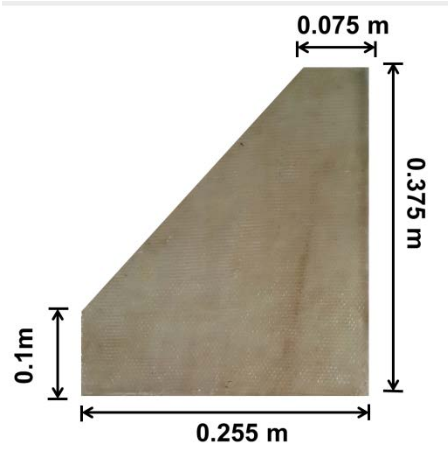


**Figure 9:** Typical [0/90] composite delta wing

Composite typical delta was manufactured by similar steps presented in figure (8). Where mold is presented in figure (7) is coated with a thin layer of separator liquid. Then fibers were cut and arranged with resin.

## 5. Experimental Setup

All mentioned wings were tested in laboratory under environment and boundary condition very similar to those used in ANSYS test. Experimentally two metal F-clamps were used with wooden frame to firmly fix tested wing, this rig gives ability to the user for changing wings when tests was finished by only opening clamped edges. Clamping system that used in experimental work is presented in figure (10) with aluminum wing.

**Figure 10:** Boundary condition of delta wing

In Experimental work two tests were performed first one was for measuring free response for each wing where full presentation of devices used in this section is stated in figures (11) for aluminum, [0/90] composite and aluminum foam wings.

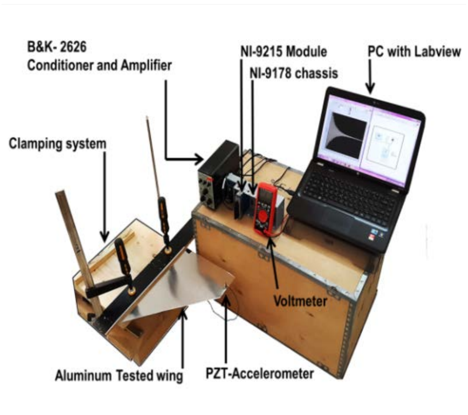


Delta wing

**Figure 11:** Recording of free responses

Calibrated accelerometer was used to sense acceleration then data transmitted to PC by converting it by PCIE- 6321 NI- USA- Data acquisition. Schematic presentation for active vibration suppression loop is presented in figure (12).

The real electrical circuit with devices that used in current work are presented in figure (13) for aluminum, [0/90] composite and aluminum foam. In mentioned figure each devices are labeled with its name to facilitate searching its specifications for interested readers

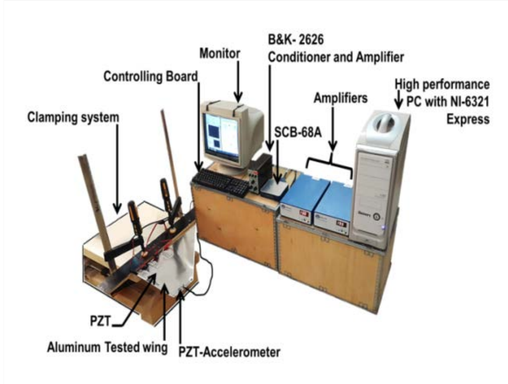


Aluminium delta wing

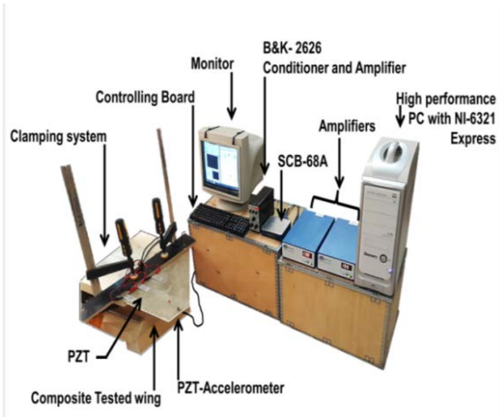


Composite delta wing

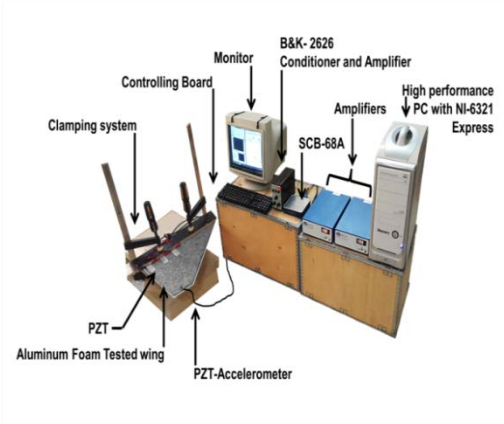


Aluminium foam delta

**Figure 13:** Experimental setup for active vibration control

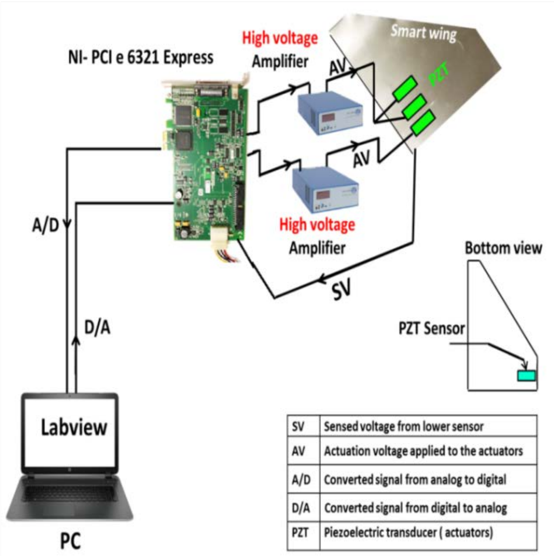


**Figure 12:** Schematic view of the experimental active vibration control setup – Delta wing

## 6. Results and Discussion

Free and actively controlled responses aluminium triangular wing are presented in figures (14) ~ (15). Both P, PI controllers are included within controlled responses. Although P controller presents noticeable enhancement for gain of 2, 4 and 8 in which 0.5, 1.5 and 2.5 Sec. from free settling time was eliminated in controlled responses, one can get further improvement in response with adding I term which will act on decreasing both settling time and response amplitude. From mentioned figures it was noticed that adding I term with gain of 4, 8 further seconds will be removed or in another word attenuated from overall settling time where 3.5sec, 4.8sec. was decreased from free settling time at mentioned gains.

Both weight and wing size plays an important rule on improvement controller performance. Also dimensional compatibility between controlled structure and actuators acts in high degree on add further ability to controller action to be noticed on final response. It was noticed that adding of I term leads to further enhancement in settling time. Amount of time decreasing was small for both P and PI, but actually it represents decreasing of 35% of the overall time of wing vibration. Figures (16), (17) present Free and actively controlled responses composite triangular wing with P and PI controllers. Enhancement in response with P controller gain of 2, 4 and 8 was 2, 3.2 and 4.1 Sec. so depending on previous results of aluminium wing, one can get further improvement in response with adding I term specially for composite wing, where it's free response was settle faster than aluminium thus will act on decreasing both settling time and response amplitude if I term be added. From mentioned figures it was noticed that adding I term with gain of 4, 8 further seconds will be removed or in another word attenuated from overall settling time where 4.5 sec, 5.1 sec. was decreased from free settling time at mentioned gains. Decreased seconds by mentioned controlling method will be very significant for real wing where each second presents a percentage ratio from total settling time. Here with composite triangular wing 51% of overall settling time was attenuated with Kp =8, Ki =4. Free and actively controlled responses of aluminium foam triangular wing are presented in figures (18) (19) where total comparison between responses with P controller are presented in figure (18). Corporation between light weight and high stiffness can be shown in foam response where P controller presents high enhancement in responses in comparison with previously tested materials. P controller with gain of 2, 4 and 8 in which 3.5, 4 and 6 sec. High improvement in response of wing will be satisfied with PI controller as stated in figure (19) where 72% of overall settling time was decrease. Free and controlled responses were measured experimentally by mentioned devices for both P and PI controller where total controller circuit was constructed by using Labview 2015. In which functional programming was activated. Figures (20), (21) and (22) show free and controlled responses measured experimentally for aluminium, [0/90] composite and aluminium foam respectively. Percentages of settling time decreasing was evaluated by comparison between free and controlled values and dividing difference between them with settling time value of free response.

## 7. Conclusions

1- The three dimensional finite element model proposed can predict accurately the free vibration and controlling response of tested aircraft wings for different material properties and different controlling type.

2-Using aluminum foam in all mentioned wing show high performance in free vibration case followed by composite then aluminum.

3-Enhancement of 35% was satisfied with PI controller for aluminum.

4- About 59% of overall response was eliminated with PI controller with composite.

5- Further 72% of free response for aluminum foam was eliminated with PI controller.

6- Using of aluminum foam adds more stability to tested wing when vibration controller turned ON.

7. Noticeable deterioration in wing's response was seemed when including derivative term so only PI terms was activated.

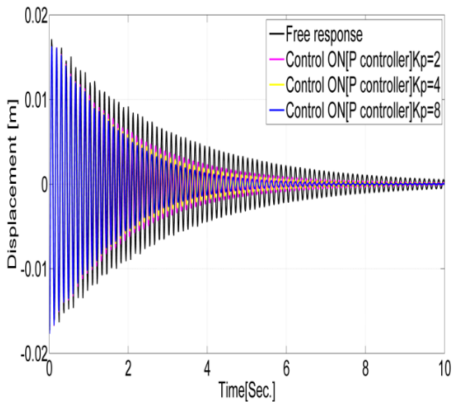


**Figure 14:** Comparison of numerically measured responses for Aluminium triangular wing with P controller.

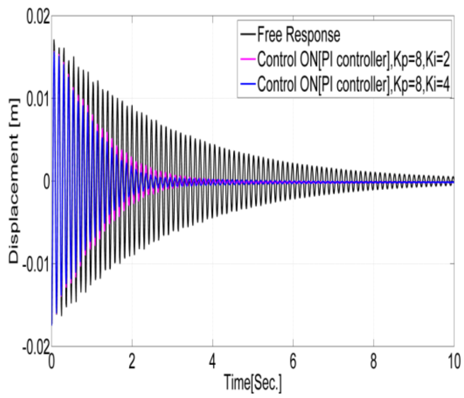


**Figure 15:** Comparison of numerically measured responses for Aluminium triangular wing with PI controller.

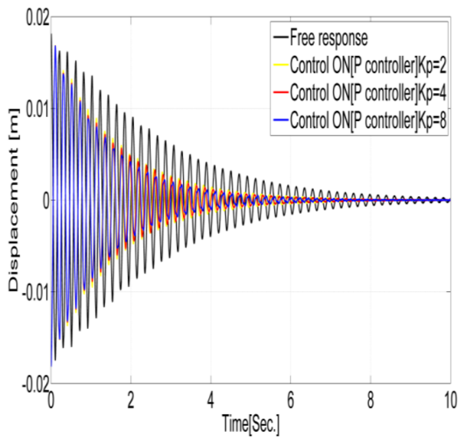


**Figure 16:** Comparison of numerically measured responses for Composite triangular wing with p controller.

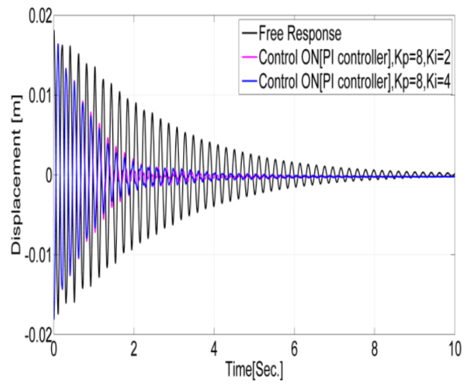


**Figure 17**: Comparison of numerically measured responses for Composite triangular wing with PI controller.

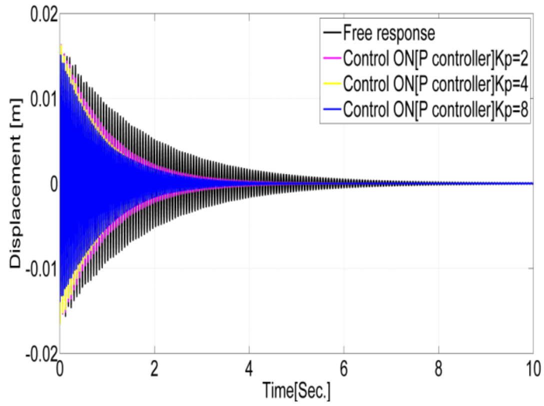


**Figure 18:** Comparison of numerically measured responses for aluminium foam triangular wing with P controller.

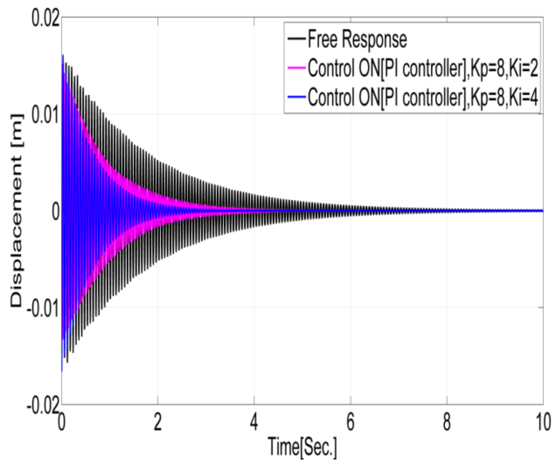


**Figure 19:** Comparison of numerically measured responses for aluminium foam triangular wing with PI controller.

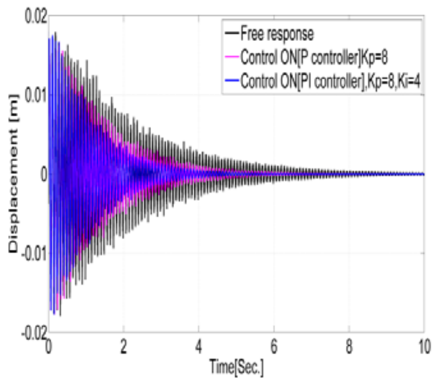


**Figure 20:** Comparison of experimentally measured responses for aluminium delta wing with P, PI controller.

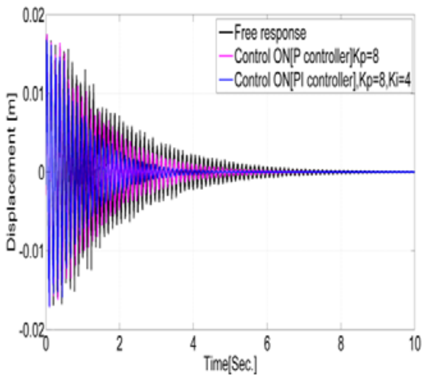


**Figure 21:** Comparison of experimentally measured responses for composite delta wing with P. PI controller.

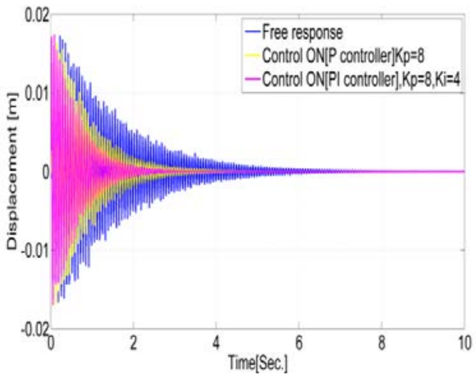


**Figure 22:** Comparison of experimentally measured responses for aluminium foam delta wing with P, PI controller.

## List of Symbols

**K:** Controller gain
**e(t):** Estimated error value
**r(t):** Reference input.
**y(t):** Measured output
**u(t):** Control signal
***Ti*:** Integral Time
**Td:** Derivative time
**PID:** Proportional- Integral- Derivative
**LQR:** Linear quadratic regulator
**dt:** Time step
**PZT:** Piezoelectric transducers
**AVC:** Active vibration control
**{T}:** Stress vector
**{S}:** Strain vector
**{D}:** Electrical displacement vector
**{E}:** Electrical field vector
**[c]:** Elasticity matrix
**[e]:** Piezoelectric matrix
**[$e^T$]:** Dielectric matrix
**[M]:** Mass matrix
**[K]:** Stiffness matrix
**[C]:** Damping matrix
**[$K^d$]:** Dielectric stiffness matrix
**{u}** Nodal displacement vector
**{v}** Electric potential vector
**{F}** Mechanical force vector
**{L}** Electrical charge vector
**Kp:** Proportional controller gain
**Ki:** Integral Controller gain

## References


1. Daniel J. Inman, “Vibration with Control”, John Wiley & Sons Ltd, England, 2006.
2. Yavuz Ş, Malgaca L, Karagülle H. , “Vibration control of a single-link flexible composite manipulator”. Composite Structures. Elsevier Ltd; vol.140, PP:684–91, 2016.
3. Chevva K, Sun F, Blanc A, Mendoza J., “Active vibration control using minimum actuation power”. Journal of Sound Vibration. Elsevier; vol.340, PP1–21, 2015.
4. Fatih M., “Active flutter suppression of smart fin”, M.Sc. thesis, Middle east university, 2008.
5. Gopinathan SV, Varadan VV, Varadan V, “A review and critique of theories for piezoelectric laminates”. Smart Material and Structures, vol.9,PP:24–48,2000. http://dx.doi.org/10.1088/0964-1726/9/1/304
6. Boudaoud H, Daya EM, Belouettar S, Duigou L, Ferry MP., “Damping analysis of bea.ms submitted to passive and active control”. Engineering Structures, vol.31, PP:322–31, 2009. http://dx.doi.org/10.1016/j.engstruct.2008.08.009
7. Hwu C, Chang WC, Gai HS., “Vibration suppression of composite sandwich beams”. Journal of Sound and Vibration , vol.272,PP:1–20,2004.

http://dx.doi.org/10.1016/S0022-460X(03)00302-X

8. Narayana.n S, Balamuruga.n V., “Finite elemen.t modeling off piezo laminated smar.t structures for active vibraton control wi.th distributed sensors and actuators”. Journal of Sound and vibration, vol.262, PP:529–62, 2003.
9. Baillargeo.n B., V.el S.S,, “Active vibration suppression of sandwich beams using piezo.electric shear actuators: experiments and numerical simulations”. Journal of Intelligent Material System and Structure, vol.16,PP:517–30, 2005. http://dx.doi.org/10.1177/1045389X05053154
10. Ahmed Abdul-hussain Ali, Hussain Yousif Mahmood, and Mahmood Wael Saeed, “Active Vibration Control of Aircraft Wing Using Piezoelectric Transducers”, International Journal of Scientific & Engineering Research, vol. 7, no. 5, May 2016.
11. Ahmed Abdul-hussain Ali, Hussain Yousif Mahmood, and Mahmood Wael Saeed, “ A Comparison between Velocity Feedback and Proportional-Integral-Derivative[PID] performance In Active Vibration Control”, Journal of Vibration Analysis, Measurement, and Control, vol. 4, no. 1, 2016.
12. Ahmed Abdul-hussain Ali, Mahmood Wael Saeed, “Active Vibration Suppression of Acrobatic Aircraft Wing by Acceleration Feedback Controller”, International Journal of Computer Applications, vol. 157, no. 10, January 2017.
13. Ahmed Abdul-hussain Ali, “Stability Improvement of an Unmanned Aerial Vehicle's Wing using Active Vibration Control”, International Journal of Computer Applications, vol. 157, no. 10, January 2017.
14. Katsuhiko Ogata, “Modern Control Engineering” .5th Edition, Pearson education Inc., 2011.
15. ANSYS user manual, ANSYS user manual (version 15.0). USA: ANSYS, Inc., 2014.
16. Iraqi Central Organization for Standardization and Quality Control (COSQC), Data Sheet with Mechanical properties of tested material, 2016.

# تخفيض الاهتزاز لجناح دلتا باستخدام المنظم التناسبي- التكاملي عمليا وعدديا

**أحمد عبدالحسين علي**
قسم الهندسة الميكانيكية
جامعة بغداد

**حسين يوسف محمود**
قسم الهندسة الميكانيكية
جامعة بغداد

**محمود وائل سعيد**
قسم الهندسة الميكانيكية
جامعة بغداد

**الخلاصة**

استخدام دائرة تخميد الاهتزاز الفعالة باستخدام المنظم التناسبي – التكاملي عمليا وعدديا لتخميد اهتزاز جناح من نوع دلتا ولثلاث انواع مختلفة من مواد التصنيع وهي الالمنيوم,(90/0) مواد مركبة و رغوة الالمنيوم. جرى اختبار كل من المنظم التناسبي و المنظم التناسبي- التكاملي بصورة منفصلة. تم اجراء الجانب العددي باستخدام برنامج انسز النسخة 15 حيث ان دائرة المنظم مع المواد الذكية كانت قد اُدخلت بملف برمجة (ماكرو). الاجنحة العملية جرى تصنيعها ليتم اختبارها تحت الاثارة الممثلة سابقا في برنامج الأنسز. تم استخدام برنامج لاب فيو النسخة 2015 مع محول اشارة عالي السرعة الى جانب مولدات الاشارة لإكمال عمل منظومة السيطرة عمليا. تم الحصول على تخميد جيد لاهتزاز الجناح حيث تم تقليل 72% من زمن اهتزاز الجناح لجناح مصنوع من رغوة الالمنيوم. تم ملاحظة توافق جيد بين الاستجابات المقاسة عمليا مع تلك المقاسة عدديا.